

This is an Accepted Manuscript version of the following article, accepted for publication in:

A. Agote, A. Arruti, I. Aizpuru and M. Mazuela, "Alternative Approach Based on Bézier Curves to Model Core Losses With the Composite iGSE Method," *2024 Energy Conversion Congress & Expo Europe (ECCE Europe)*, Darmstadt, Germany, 2024, pp. 1-6.

DOI: <https://doi.org/10.1109/ECCEurope62508.2024.10751923>

© 2024 IEEE. Personal use of this material is permitted. Permission from IEEE must be obtained for all other uses, in any current or future media, including reprinting/republishing this material for advertising or promotional purposes, creating new collective works, for resale or redistribution to servers or lists, or reuse of any copyrighted component of this work in other works.

Alternative Approach Based on Bézier Curves to Model Core Losses With the Composite iGSE Method

Anartz Agote

*Electronics and Computing Department
Mondragon Unibertsitatea
Hernani, Spain
anartz.agote@alumni.mondragon.edu*

Asier Arruti 

*Electronics and Computing Department
Mondragon Unibertsitatea
Hernani, Spain
aarruti@mondragon.edu*

Iosu Aizpuru 

*Electronics and Computing Department
Mondragon Unibertsitatea
Hernani, Spain
iaizpuru@mondragon.edu*

Mikel Mazuela 

*Electronics and Computing Department
Mondragon Unibertsitatea
Hernani, Spain
mmazuela@mondragon.edu*

Abstract- This work addresses limitations of the composite improved generalized Steinmetz equation for core loss calculation and presents a more robust definition of the losses. First, the limitations due to extrapolation of the fifth-degree polynomial functions used in the previous work are presented, resulting in inaccurate predictions in certain cases. As a solution, Bézier curves are proposed, which can accurately model the loss transition from low frequency (hysteresis loss) to high frequency (eddy loss), while remaining tangential outside of the parametrization range. The presented approach is not only more robust, but also requires less parameters to define the losses, while retaining similar or better accuracy than the approach.

Index Terms- Core loss, Magnetic cores, Ferrites, Curve fitting, Numerical analysis.

I. INTRODUCTION

Transformers and inductors are one of the key components for on power converters, playing major roles in the efficiency, power density, weight, and cost of the design [1]-[4]. Thus, the meticulous design of these devices for the requirements of each specific application is critical to achieve high performance power converters.

Regarding switch mode power supplies (SMPS), the size of magnetics has been decreased with the adoption of wide band gap (WBG) transistors allowing to push higher frequencies. Unfortunately, the optimal design of high frequency magnetics is a challenging endeavour, with smaller cores resulting in decreased cooling capabilities, giving rise to higher temperatures [5]. Thus, the capacity to predict the magnetic device losses and temperatures accurately becomes more important than ever.

Focusing on the core losses, various approaches exist, starting from the Steinmetz Equation [6]. This approach can

predict the losses of sinusoidal waveforms accurately, but triangular waveforms are often more common in SMPS. The improved generalized Steinmetz equation (iGSE) proposes an alternative for non-sinusoidal waveforms [7], but it has been demonstrated that the accuracy is not adequate for all duty cycles [8]. To improve the accuracy of the iGSE, the composite improved generalized Steinmetz equation (ciGSE) is proposed in [8], which combines the key concepts of both the composite waveform hypothesis (CWH) [9] and the iGSE, extracting the necessary parameters directly from triangular waveforms of variable duty cycles.

Once all the necessary parameters are obtained, the triangular waveform losses can be obtained by evaluating the losses of each segment (i) using

$$P_i = \exp(g(\ln(\Delta B), \ln(dB/dt))), \quad (1)$$

and then adding them together in the same manner as the CWH approach

$$P_{\text{loss}} = \sum D_i \cdot P_i. \quad (2)$$

Although the ciGSE was proved to offer noticeable improvements regarding previous models in a wide range of frequency, flux density and duty cycle based on the MagNet database [10]-[13]. The implementation of the fifth-degree polynomials to define the loss space function (1) reported inaccurate results when extrapolation is required [8]. This is an innate limitation of high-degree polynomial fitting, which becomes divergent at the boundary of the fitting dataset, resulting in the function quickly shooting to $\pm\infty$ outside the fitting boundary. Since the ciGSE polynomial fitting methodology is incapable of using data from all duty cycles, evaluation of losses at extreme duty cycles ($D=0.1$ and $D=0.9$) requires extrapolation. In addition, if the ciGSE is evaluated outside of its fitting boundaries $f \notin [55 \text{ 445}] \text{ kHz}$ $D \notin [0.1,$

This work was supported by the Department of Education of the Basque Government under the Non Doctoral Research Staff Training Program through grant PRE_2020_1_0267. (Corresponding author: Anartz Agote)

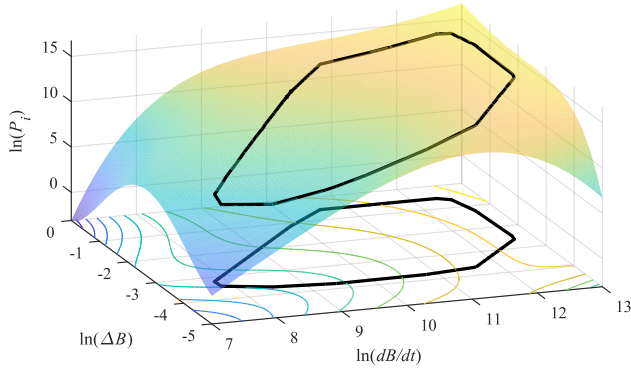


Fig. 1: Visualization of the ciGSE loss space defined by fifth-degree polynomials and its parametrization boundaries for N87 at 25 °C. Notice how the tendencies inside and outside the boundaries are not the same, resulting in the extrapolation.

0.9] a loss in precision is unavoidable. This is illustrated in Fig. 1, with the predicted losses quickly increasing outside of the parametrized loss space boundaries.

This work will address this problem by presenting an alternative approach to model the loss space function (1) based on Bézier curves. As will be demonstrated, the Bézier curve allows to describe the curvature of the loss space while remaining tangential outside of the parametrization range. Due to this tangentiality, the new approach better describes the hysteresis and eddy loss phenomena that govern the losses in low and high frequency ranges, resulting in an improved extrapolation performance and a much-increased accuracy on those cases.

First, **SECTION II** will present an introduction to Bézier curves, demonstrating the key properties of continuity and tangentiality. Then, **SECTION III** discusses the implementation of these Bézier curves as an alternative to the fifth-degree polynomial functions used for the loss space definitions. Lastly, **SECTION IV** presents the obtained results, demonstrating the improvement in accuracy due to a better extrapolation process.

II. BÉZIER CURVES

Bézier curves are parametric curves commonly used in computer graphics to describe paths using a set of control points [14]. The curve is defined by a mathematical function, which for the cubic Bézier curves used in this work takes the matrixial representation

$$f(t) = \begin{bmatrix} t^3 & t^2 & t & 1 \end{bmatrix} \begin{bmatrix} -1 & 3 & -3 & 1 \\ 3 & -6 & 3 & 0 \\ -3 & 3 & 0 & 0 \\ 1 & 0 & 0 & 0 \end{bmatrix} \begin{bmatrix} P_0 \\ P_1 \\ P_2 \\ P_3 \end{bmatrix}, \quad (3)$$

with P_0, P_1, P_2 and P_3 being the control points and t used to define the position inside the curve (ranging from 0 to 1). At its extremes, a Bézier curve shows a G^1 continuity (tangent continuity) with the lines defined by the P_0 and P_1 control points ($t = 0$) and the P_2 and P_3 points ($t = 1$).

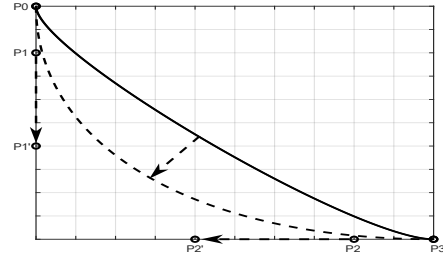


Fig. 2: Demonstration of the effect of the control points in a cubic Bézier curve.

As illustrated in Fig. 2, the control points give complete freedom when defining the geometry of the Bézier curve, allowing to adjust the edge points, curvature, and tangents of the curve. Thus, due to the tangent continuity properties and the capabilities to control the curvature, Bézier curves are ideal candidates to achieve similar results to fifth-degree polynomials while retaining good extrapolation capabilities when the tangents are set correctly.

Lastly, the matrixial form of a Bézier curve is very similar to the equations employed in the ciGSE [8], which allows to use the Steinmetz parameter extraction techniques described in that work. Retaining the capability to obtain the Steinmetz parameters of a specific point, since many other works tackling the problem of core losses make heavy use of this, allows to combine the Bézier curve approach with those presented in works regarding the impact of relaxation [15] and influence of pre-magnetization [16] in the core losses.

III. IMPLEMENTATION

Although the Bézier curves appear to solve all the main issues of the fifth-degree polynomials approach, there is still a huge issue in their implementation of the problem of core losses: the cubic Bézier curves are only applicable to two dimensional problems, while the core losses are a three-dimensional problem: $x = \ln(dB/dt)$, $y = \ln(\Delta B)$, and $z = \ln(P_i)$.

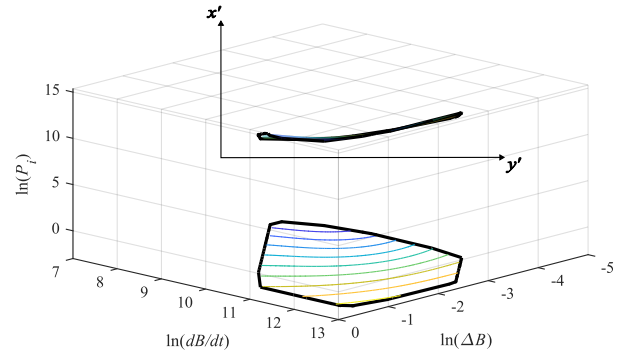


Fig. 3: Rotated ciGSE loss space Fig. 1 into a two-dimensional problem for N87 at 25 °C. There it can be seen how the surface looks like a 2D curve. For the 2D representation a new perspective axis (x' and y') will be defined. Theoretically this remains being a 3D problem but one of the axes is not appreciable.

Fortunately, in all cases tested, the ciGSE loss space shown in Fig. 1 (when confined to its boundaries, no extrapolation) resembles a two-dimensional problem when the xyz axis are rotated accordingly, as illustrated in Fig. 3.

This can be done by applying the rotational matrixes (notice that the rotations are applied by multiplying the data by these matrixes)

$$R_x = \begin{bmatrix} 1 & 0 & 0 \\ 0 & \cos \theta_x & -\sin \theta_x \\ 0 & \sin \theta_x & \cos \theta_x \end{bmatrix}, \quad (4)$$

$$R_y = \begin{bmatrix} \cos \theta_y & 0 & \sin \theta_y \\ 0 & 1 & 0 \\ -\sin \theta_y & 0 & \cos \theta_y \end{bmatrix}, \quad (5)$$

$$R_z = \begin{bmatrix} \cos \theta_z & -\sin \theta_z & 0 \\ \sin \theta_z & \cos \theta_z & 0 \\ 0 & 0 & 1 \end{bmatrix}, \quad (6)$$

where the R_n matrix rotates the xyz data along the i (x , y or z) axis. Note that although three rotational matrixes can be described, only two rotations are necessary to fully rotate a three-dimensional space.

The initial three-dimensional space where $x = \ln(dB/dt)$, $y = \ln(\Delta B)$, and $z = \ln(P_i)$ is transformed into the new x' , y' and z' coordinates. These new dimensions are linear combinations of the initial xyz system, but unlike the original system they will lose direct physical interpretability (dB/dt , ΔB , P_i). The rotation process is completely reversible, hence, going in the opposite direction, an $x'y'z'$ datapoint can be transformed into its xyz counterpart, restoring the physical interpretability.

Once the problem has been simplified to two dimensions, the control points that will define the Bézier curve can be defined. This is done using a multivariable non-linear programming solver, which in this case is MATLAB's `fminunc` function. This solver will adjust the control points, and in turn

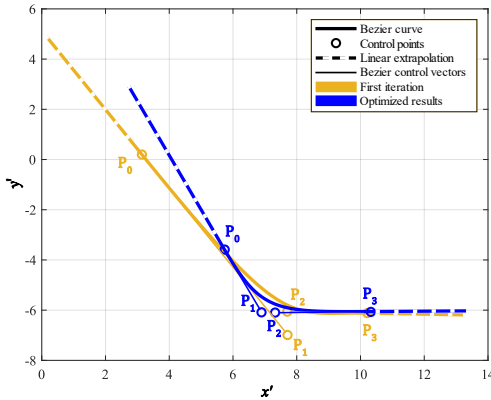


Fig. 4: First iteration and last iteration Bézier curves for N87 at 25 °C. It can be seen how outside the P_0 and P_3 limits the Bézier curve becomes a linear function, resulting in linear extrapolation.

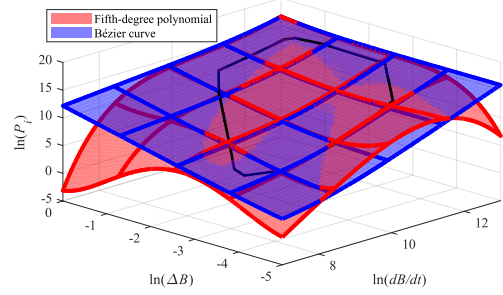


Fig. 5: Comparison of the fifth-degree polynomial and Bézier curves outside of the parametrization boundaries (extrapolation) for N87 at 25 °C. The fifth-degree polynomial surface goes $\pm\infty$ on the outside of the parametrization boundaries, while the Bézier curve follows the tendency.

adjust the shape of the Bézier curve to better fit the experimental data from the MagNet database [10]-[13].

The optimizer will use $\ln(dB/dt)$ and $\ln(\Delta B)$ as set inputs, and modify the P_0 , P_1 , P_2 and P_3 control points. For each set of points, the Bézier is rotated back into the xyz coordinates, allowing to evaluate (1) and (2) to get a core loss prediction for each waveform. Then, the results are compared against the empirical data, obtaining the root mean relative error, which is the parameter the optimizer will try to minimize. The optimizer will iteratively repeat these steps until it finds a point where fine tuning the control points makes no further improvements. The characterization of the initial parameters is approximated from the shape of the fifth-degree polynomials (rotation angles and control points). Comparison of the Bézier curves obtained in the first iteration and final iteration are shown in Fig. 4.

In total, there are ten parameters required to define the $x'y'z'$ Bézier curve: $P_{0,x'}$, $P_{0,y'}$, $P_{1,x'}$, $P_{1,y'}$, $P_{2,x'}$, $P_{2,y'}$, $P_{3,x'}$, $P_{3,y'}$, and two angles to rotate back into the original xyz dimensions, in this case θ_x and θ_y . These 10 parameters are less than half of the 21 required in the fifth-degree polynomials of the original ciGSE publication [8], resulting in a more compact model.

To demonstrate the improved extrapolation, Fig. 5 displays the loss space used in the original ciGSE expanded beyond its boundaries, compared against the Bézier curve expanded to the same range.

IV. OBTAINED RESULTS

To evaluate the new approach, the same concept presented in [8] is followed, the experimental data available on the MagNet database [10]-[13] for triangular waveforms will be used. This includes 10 materials at 4 different temperatures, with frequencies ranging from 55 kHz up to 445 kHz, peak to peak flux densities ΔB up to 500 mT and duty cycles D from 0.1 up to 0.9.

The ciGSE loss space methodologies are evaluated with the fifth-degree polynomials as presented in the original work [8] and with the Bézier curve approaches. First, both approaches are tested considering all the data points.

In general, for materials with many available waveforms, the parametrization can be done in a wide range, and thus extrapolation is only required in less than 5 % of the data. Still, in the case of materials with a lesser number of datapoints, such as the 3E6 material, the reduced number of datapoints results in a tight parametrization boundary, and extrapolation is necessary for more than 5 % of the waveforms. In this work two metrics will be used to compare the performance of both fifth-degree polynomial and Bézier approaches, the root mean square relative error and the 95th percentile. Although the 95th percentile falls inside the non-extrapolation required range, this metric has been selected for two main reasons: the 95th percentile is a common metric used in the works regarding the MagNet database [10]-[13], and to keep consistency with the previous ciGSE work [8].

The results for all the cases are displayed in TABLE I. At first glance, the performance of the Bézier approach is similar to the fifth-degree polynomials approach, trading blows in certain specific materials. Nevertheless, one should remember that the newly proposed approach only requires 10 total parameters, 8 to define the control points of the Bézier curves and 2 to define the rotation angles. Thus, the Bézier approach performs slightly better while offering a much more compact model. The Bézier approach has a worst-case scenario of root mean square relative error of 8.42% (material 3F4 at 70 °C) and a 95th percentile of 18.10% (material 49 at 50 °C). In contrast, the fifth-degree polynomial approach shows higher values, with

a worst-case scenario of root mean square relative error of 42.64% (material 3E6 at 70 °C) and a 95th percentile of 33.80% (material 3E6 at 50 °C). On average, taking the root mean square relative error and the 95th percentile into account, the new approach performs 1.58 and 1.50 times better than the approach from [8], and is more consistent with the performance between different materials and temperatures.

On the opposite, as displayed by TABLE II, if only the extrapolation is considered, the Bézier approach performs much better. The performance comparison between both approaches depends on the materials. However, the further the data is from the fitting region, the more significant the improvements observed with the Bézier approach. Similarly to the previous scenario, the Bézier approach is much more consistent than the polynomials approach, with worst case scenarios of 12.88 % (material N27 at 25 °C) and 26.81 % (material 3F4 at 70 °C), while for the polynomials approach these are as high as 41.97 % (material 3C94 at 25 °C) and 92.61 % (material 3E6 at 25 °C). In this case, taking the root mean square relative error and the 95th percentile into account, the new approach performs 2.80 and 3.56 times better than the approach from [8].

TABLE I
ACCURACY OF THE ciGSE WITH POLYNOMIAL [8] AND BÉZIER APPROACHES (WITH EXTRAPOLATION)

Material	Temp. [°C]	Error RMS [%]		Error 95 percentile [%]		Data points
		polynom	Bézier	polynom	Bézier	
N87	25	2.77	5.91	5.62	11.80	3312
	50	4.00	5.16	8.10	10.14	3299
	70	6.12	5.45	13.69	10.46	3304
N49	90	9.07	6.36	21.52	11.73	3275
	25	6.75	7.02	14.76	12.00	708
	50	11.04	8.38	14.06	18.10	682
N27	70	9.04	8.20	13.01	16.35	705
	90	9.75	7.87	12.21	15.53	744
	25	5.78	5.51	9.74	11.19	886
3C94	50	8.86	5.08	15.00	10.34	888
	70	7.83	5.71	17.10	10.96	885
	90	8.97	6.82	18.63	12.71	883
3C90	25	11.38	4.87	16.30	10.03	3165
	50	11.65	4.86	16.96	9.94	3162
	70	8.84	5.02	15.16	9.61	3148
3E6	90	7.33	5.80	16.86	10.80	3152
	25	3.67	4.94	6.70	10.13	3302
	50	5.49	5.05	10.89	9.77	3286
3F4	70	7.99	6.14	19.38	11.77	3273
	90	10.70	7.18	25.07	12.87	3262
	25	16.21	1.25	33.80	2.43	515
77	50	8.30	1.67	7.08	3.24	516
	70	42.64	2.08	31.87	4.08	512
	90	7.17	2.93	7.37	5.43	502
78	25	7.07	7.74	9.07	14.29	617
	50	10.44	8.26	11.77	16.43	573
	70	15.58	8.42	17.32	16.40	562
N30	90	9.36	8.14	13.84	15.60	562
	25	6.75	6.13	10.72	12.50	883
	50	10.32	5.47	16.03	10.94	882
77	70	11.86	5.98	24.96	11.37	884
	90	13.10	7.05	30.86	13.16	879
	25	7.38	5.52	13.07	11.10	881
78	50	9.67	5.62	23.46	11.17	880
	70	13.34	6.51	30.45	11.75	882
	90	13.96	7.53	33.05	14.01	881
N30	25	5.32	3.23	5.63	6.00	678
	50	6.03	3.27	8.21	6.27	678
	70	18.17	3.00	11.88	6.00	674
90	24.29	3.05	14.06	5.90	661	
OVERALL		8.67	5.63	15.49	10.90	54270

TABLE II
ACCURACY OF THE ciGSE WITH POLYNOMIAL [8] AND BÉZIER APPROACHES (ONLY EXTRAPOLATION)

Material	Temp. [°C]	Error RMS [%]		Error 95 percentile [%]		Data points
		polynom	Bézier	polynom	Bézier	
N87	25	8.35	10.24	15.57	19.85	72
	50	2.72	6.94	5.42	15.29	66
	70	2.40	3.83	5.56	6.29	66
N49	90	3.59	6.21	6.90	10.35	64
	25	20.96	11.66	49.53	23.04	46
	50	7.84	7.06	20.55	17.61	51
N27	70	6.63	8.80	13.06	17.65	49
	90	6.99	8.31	9.02	16.40	56
	25	19.50	9.04	41.55	16.92	65
3C94	50	8.16	6.01	18.46	11.70	69
	70	18.12	9.23	41.40	17.39	68
	90	13.67	7.92	37.60	16.82	69
3C90	25	41.97	7.44	89.42	13.19	218
	50	38.77	7.70	89.49	14.14	213
	70	11.84	4.66	22.68	10.02	212
3E6	90	30.20	5.91	73.24	12.26	214
	25	13.01	9.06	23.28	15.20	130
	50	4.32	5.07	8.99	10.85	127
3F4	70	3.75	4.39	7.95	9.70	129
	90	6.69	5.92	15.83	12.15	131
	25	35.62	1.25	92.61	2.19	106
77	50	26.38	1.07	77.26	2.09	111
	70	35.34	1.35	92.61	2.42	103
	90	20.87	1.31	53.74	2.38	102
78	25	27.66	12.88	71.62	24.43	29
	50	4.45	5.84	9.13	8.36	30
	70	5.11	9.99	11.14	26.81	39
N30	90	5.43	5.63	11.42	10.93	27
	25	22.51	9.91	45.85	18.65	65
	50	22.20	9.14	45.96	18.69	63
77	70	18.93	8.99	40.92	16.27	67
	90	18.18	8.88	42.29	16.48	62
	25	24.43	8.31	48.35	14.76	67
78	50	21.29	7.20	47.89	16.55	66
	70	22.68	7.39	48.35	14.17	67
	90	22.69	7.55	48.35	14.77	67
N30	25	13.03	2.92	34.30	5.40	103
	50	9.85	2.75	22.75	5.47	114
	70	11.35	3.56	25.92	6.82	108
90	8.80	2.83	19.76	5.69	117	
OVERALL		18.48	6.02	42.53	11.77	3628

V. CONCLUSIONS

This work is a continuation of the composite improved Generalized Steinmetz Equation presented in [8], addressing the problems generated due to extrapolation with fifth-degree polynomials.

As alternative to the fifth-degree polynomials, Bézier curves are presented due to their capacity to modify the curvature to fit the existing datasets, while retaining G^1 continuity (tangent continuity) in the extremes, resulting in a better extrapolation performance.

To implement the two-dimensional Bézier curves to model the three-dimensional loss spaces, these are rotated twice (z and x axes). This transforms the loss space into an x' and y' two-dimensional problem, where a multivariable non-linear solver can be used to obtain the definitions of the Bézier curves.

When comparing the fifth-degree polynomials approach with the Bézier curves, when extrapolation is not required, the Bézier approach is slightly less accurate, but more consistent across the different materials and temperatures. On the contrary, when extrapolation is required, the Bézier approach performs much better while still retaining consistent results. Considering that the Bézier approach also requires less parameters than the polynomials (10 instead of 21), the new proposed approach can be considered an improved version of the fifth-degree polynomials approach.

ACKNOWLEDGMENTS

The authors would like to thank all people behind the generation and maintenance of the MagNet database.

DATA AVAILABILITY

All the experimental data used to support this study is available at MagNet [10]-[13].

All the parameters required to implement the Bézier curves can be found in TABLE IV.

APPENDIX A: IMPLEMENTATION OF THE MODEL

To implement the code from TABLE III and predict the losses in the magnetic core of a material with known parameters, the following method is proposed. First, the 2D curve is created from equation (3) and extended through the third dimension, resulting in an overlapping surface. To do so, the parameters $P_{\theta X}$, $P_{\theta Y}$, P_{1X} , P_{1Y} , P_{2X} , P_{2Y} , P_{3X} and P_{3Y} , are replaced by the parameters $P_{0,x'}$, $P_{0,y'}$, $P_{1,x'}$, $P_{1,y'}$, $P_{2,x'}$, $P_{2,y'}$, $P_{3,x'}$, $P_{3,y'}$ given in the TABLE IV.

In this way, a grid of points is created, defining a plane. The coordinates of the points are stored in a matrix (bez), which allows the generated plane to be rotated to the real axes of $\ln(dB/dt)$, $\ln(\Delta B)$, and $\ln(P_i)$. For this purpose, multiplications with the matrices (rotM1 and rotM2) of equation (4) and (5) are performed, replacing thx and thy by θ_x and θ_y .

Once the plane is in the original axes, the losses of each segment of the wave are searched on the plane on specific dBdt and DB. Finally, the concept of composite (2) is applied to obtain the total losses.

REFERENCES

- [1] J. W. Kolar et al, "PWM Converter Power Density Barriers," *Power Conversion Conference - Nagoya*, Nagoya, Japan, 2007, pp. P-9-P-29,
- [2] J. W. Kolar et al., "Exploring the pareto front of multi-objective single-phase PFC rectifier design optimization - 99.2% efficiency vs. 7kW/din3 power density," *IEEE 6th International Power Electronics and Motion Control Conference*, 2009.
- [3] J. Mühlethaler et al, "Loss modeling of inductive components employed in power electronic systems," *8th International Conference on Power Electronics - ECCE Asia*, 2011.
- [4] J. W. Kolar et al, "The ideal switch is not enough," *28th International Symposium on Power Semiconductor Devices and ICs (ISPSD)*, 2016
- [5] W. . -J. Gu et al, "A study of volume and weight vs. frequency for high-frequency transformers," *Proceedings of IEEE Power Electronics Specialist Conference*, 1993.
- [6] S. A. Mulder, "Fit Formulae for Power Loss in Ferrites and their Use in Transformer Design," in *proc. 26th International Power Conversion Conferenc*, 1993.
- [7] K. Venkatachalam, C. R. Sullivan, T. Abdallah and H. Tacca, "Accurate prediction of ferrite core loss with nonsinusoidal waveforms using only Steinmetz parameters," *2002 IEEE Workshop on Computers in Power Electronics*, 2002.
- [8] A. Arruti et al, "The Composite Improved Generalized Steinmetz Equation (ciGSE): An Accurate Model Combining the Composite Waveform Hypothesis With Classical Approaches," in *IEEE Transactions on Power Electronics*, vol. 39.

TABLE III
MATLAB CODE TO IMPLEMENT THE MODEL

```

bezurfacex = linspace(0,100,500);
t = 0:0.01:1;
bezurfacex = P_1X*(3*t.^3-6*t.^2+3*t)-P_0X*(t.^3-3*t.^2+3*t-1)+P_2X*(-3*t.^3+3*t.^2)+P_3X*t.^3;
bezurfacex = P_1Y*(3*t.^3-6*t.^2+3*t)-P_0Y*(t.^3-3*t.^2+3*t-1)+P_2Y*(-3*t.^3+3*t.^2)+P_3Y*t.^3;
bezurfacex = [bezurfacex(1)-3,bezurfacex,bezurfacex(end)+3];
bezurfacex = [(P_1Y-P_0Y)/(P_1X-P_0X)*-3+bezurfacex(1),bezurfacex,(P_3Y-P_2Y)/(P_3X-P_2X)*+3+bezurfacex(end)];
bez(:,1) = repmat(bezurfacex',length(bezurfacex),1);
bez(:,3) = repmat(bezurfacex',length(bezurfacex),1);
bez(:,2) = repelem(bezurfacex',length(bezurfacex));
rotM1=[+cos(thx),-sin(thx),0; +sin(thx),+cos(thx),0; 0,0,1];
rotM2=[+cos(thy),0,+sin(thy); 0,1,0; -sin(thy),0,+cos(thy)];
surface = bez*rotM1;
surface2 = surface*rotM2;
F = scatteredInterpolant(surface2(:,1),surface2(:,2),surface2(:,3));
for j = 1:height(dBdt)
    Z_est1(j,:) = F(log(dBdt(j,:)),log(DB));
end
Z_est(isnan(Z_est)) = 0;
P_loss = sum(exp(Z_est).*D);

```

[9] C. R. Sullivan, J. H. Harris, E. Herbert, "Core loss predictions for general PWM waveforms from a simplified set of measured data," in *proc. IEEE Applied Power Electronics Conference and Exposition (APEC)*, 2010.

[10] L. Clavero et al, "Improved Analytical Core Temperature Prediction Based on Estimation of the Non-Uniform Flux Distribution," *2023 25th European Conference on Power Electronics and Applications (EPE'23 ECCE Europe)*, 2023.

[11] D. Serrano et al., "Why MagNet: Quantifying the Complexity of Modeling Power Magnetic Material Characteristics," in *IEEE Transactions on Power Electronics*.

[12] H. Li et al., "How MagNet: Machine Learning Framework for Modeling Power Magnetic Material Characteristics," in *IEEE Transactions on Power Electronics*.

[13] H. Li et al, "MagNet-AI: Neural Network as Datasheet for Magnetics Modeling and Material Recommendation," in *IEEE Transactions on Power Electronics*.

[14] Mortenson, Michael E., "Mathematics for Computer Graphics Applications," Industrial Press Inc. p. 264. ISBN: 9780831131111.

[15] J. Mühlethaler, J. Biela, J. W. Kolar and A. Ecklebe, "Improved core loss calculation for magnetic components employed in power electronic system," *2011 Twenty-Sixth Annual IEEE Applied Power Electronics Conference and Exposition (APEC)*, DOI: 10.1109/APEC.2011.5744829.

[16] J. Mühlethaler, J. Biela, J. W. Kolar and A. Ecklebe, "Core Losses Under the DC Bias Condition Based on Steinmetz Parameters," in *IEEE Transactions on Power Electronics*, vol. 27, no. 2, pp. 953-963, Feb. 2012, DOI: 10.1109/TPEL.2011.2160971.

TABLE IV
VALUES USED FOR THE BÉZIER CURVE PARAMETERS

Material	Temp. [°C]	$P_{0,x}$	$P_{0,y}$	$P_{1,x}$	$P_{1,y}$	$P_{2,x}$	$P_{2,y}$	$P_{3,x}$	$P_{3,y}$	θ_x	θ_y
N87	25	5.7391	-3.5867	6.8938	-6.0870	7.3215	-6.0961	10.3246	-6.0706	69.1198	67.8429
	50	4.8612	-3.9287	6.3121	-5.5392	6.0713	-5.9281	9.5325	-5.4661	72.4224	66.5237
	70	3.9286	-3.7865	5.8142	-5.7788	5.4074	-5.6018	8.2823	-5.4247	75.1502	66.0665
N49	90	3.0939	-3.7658	5.2729	-5.8771	4.7275	-5.4165	7.2791	-5.3540	77.7609	65.8059
	25	4.8855	-5.1467	5.2328	-5.5469	5.6800	-7.1767	7.7732	-6.1026	75.8926	67.4699
	50	4.4910	-5.1610	4.9782	-5.6242	5.0687	-7.0936	7.2509	-6.2147	77.1117	67.5872
N27	70	4.4088	-5.0434	5.1215	-5.5898	4.9284	-7.2438	7.8762	-5.9305	77.2225	67.5482
	90	4.5955	-4.9199	5.3138	-5.3343	5.2024	-7.1698	8.0925	-5.9037	76.4815	67.5429
	25	5.3029	-3.4566	7.3656	-6.0867	7.2800	-5.8012	10.3896	-5.9156	69.2620	66.9968
3C94	50	4.3038	-4.2135	6.2547	-4.8648	5.0605	-6.0028	9.5982	-5.3160	73.5614	65.8915
	70	3.2603	-3.9059	5.5325	-5.5141	4.5405	-5.5387	8.0253	-5.3226	76.9687	65.4898
	90	2.5660	-3.8950	5.3580	-5.5428	3.9514	-5.4798	7.1128	-5.3249	78.6908	65.4322
3C90	25	4.9689	-3.4497	6.6795	-6.1817	7.2484	-5.6501	10.1606	-5.7066	70.8012	66.2810
	50	3.5484	-3.3801	5.3954	-5.6595	5.3505	-5.5426	8.3982	-5.3717	75.2513	65.3867
	70	2.5803	-3.2750	4.3642	-5.8233	4.6240	-5.3445	6.8977	-5.3369	78.6951	65.0309
3E6	90	-1.9465	-3.2317	3.5615	-5.9713	4.1271	-5.3365	6.0224	-5.3479	81.1780	65.0559
	25	5.2012	-3.7388	6.6689	-6.2937	7.1370	-5.8878	9.7566	-5.8330	71.1699	66.8358
	50	4.1615	-3.7387	5.8131	-6.0712	5.8447	-5.6400	8.3965	-5.5412	74.7049	66.0069
3F4	70	3.3427	-3.7062	5.1317	-6.1265	5.0060	-5.5809	7.2320	-5.5365	77.3234	65.8753
	90	2.7458	-3.7551	4.6459	-6.1330	4.4239	-5.5847	6.4114	-5.5443	79.3129	65.8785
	25	4.2243	2.0707	1.8827	-6.4560	6.6706	-4.2225	8.9609	-4.7575	75.4014	63.3406
77	50	2.9247	-1.6041	5.3964	-4.3980	5.0308	-4.3981	9.4670	-4.4902	73.3435	62.9580
	70	1.4264	0.5055	6.3202	-4.5251	5.1973	-4.3028	10.4244	-4.4957	70.6461	62.9889
	90	2.5025	-1.6755	6.9215	-5.1643	6.8695	-4.1269	10.3368	-4.5963	71.3051	63.0735
78	25	5.5211	-3.2084	5.7949	-7.1829	8.5199	-8.6536	10.7660	-5.9271	71.5757	70.8268
	50	5.2621	-4.6082	6.4305	-6.7118	6.9017	-7.1532	8.7123	-6.5080	73.6230	69.0081
	70	5.2520	-4.9036	5.7252	-5.2614	6.0529	-7.4089	8.5249	-6.0008	74.7972	68.0315
N30	90	5.1188	-4.7167	5.6815	-5.2275	5.6612	-6.8213	8.3305	-5.7190	75.7895	66.9716
	25	5.3320	-3.7053	7.1669	-5.8813	7.1281	-5.9090	10.5850	-5.7596	69.4201	66.8306
	50	3.9689	-3.7467	6.3352	-5.3760	5.5852	-5.7742	9.2110	-5.3832	73.1817	65.8726
N30	70	2.8307	-3.8601	5.2336	-5.6325	4.4620	-5.5734	7.6585	-5.3342	77.5248	65.5789
	90	2.1165	-3.9203	4.7556	-5.7005	3.8322	-5.5070	6.7154	-5.3312	79.8597	65.5195
	25	5.1349	-4.2347	6.9076	-5.3017	6.1091	-6.0600	10.2174	-5.5862	70.9036	66.5823
N30	50	3.7737	-4.0712	6.0436	-5.4635	4.9786	-5.7174	8.6569	-5.3961	74.9522	65.8585
	70	2.6901	-3.8314	5.0413	-5.8628	4.4014	-5.5164	7.2761	-5.4013	78.3961	65.7120
	90	2.1240	-3.8889	4.9249	-5.8156	3.8677	-5.5052	6.6282	-5.3990	79.7837	65.6653
N30	25	2.7119	-2.2919	4.1502	-4.6404	3.9475	-4.8862	7.1703	-4.8284	78.9221	63.8312
	50	2.7177	-2.3260	4.7143	-4.5492	4.2544	-4.6975	7.9731	-4.6787	77.9210	63.5422
	70	2.4222	-2.0233	4.7024	-4.5892	4.5544	-4.4759	7.8878	-4.5619	77.9856	63.2004
	90	1.3336	-1.7463	4.8554	-4.7151	4.5213	-4.1591	7.6585	-4.4106	79.3049	62.6711